Raman Spectral Evidence for a μ-Oxo Bridge in the Binuclear Iron Center of Ribonucleotide Reductase†

Britt-Marie Sjöberg,* Thomas M. Loehr, and Joann Sanders-Loehr

ABSTRACT: The Raman spectrum of the B2 subunit of *Escherichia coli* ribonucleotide reductase shows a peak at 496 cm^{-1} that appears to be in resonance with the 370-nm electronic transition of the binuclear iron center in both the native and radical-free forms of the protein. Exposure of the protein to $H_2{}^{18}O$ causes the peak to shift to 481 cm^{-1}, indicating that the vibrational mode is due to an Fe–O moiety in which the oxygen can exchange with solvent. The rate of oxygen exchange (k_{obsd} = 8.3 × 10^{-4} s^{-1}) is consistent with a μ-oxo-bridged structure. Protonation of the oxygen is unlikely since the Fe–O vibration fails to shift to lower frequency in D_2O. Instead, there is a gradual increase in the vibrational frequency with time to a maximum value of 502 cm^{-1} after 3 h in 70% D_2O. Apparently, the deuteration of successive protein functional groups causes a slight alteration in the structure of the binuclear iron center. The resonance Raman characteristics of the Fe–O–Fe group in protein B2 are similar to those previously reported for the μ-oxo-bridged binuclear iron center in hemerythrin. A further similarity between the two proteins is the high degree of α-helical content. Circular dichroism measurements place this value at ~60% for the B2 subunit of ribonucleotide reductase.

The enzyme ribonucleotide reductase catalyzes the reduction of ribonucleotides to their corresponding deoxyribonucleotides (Thelander & Reichard, 1979). Since this is the first committed step in the formation of deoxyribonucleotides, ribonucleotide reductase is also a key control point for the regulation of DNA[1] biosynthesis. The *Escherichia coli* enzyme is composed of two subunits, proteins B1 and B2, which are required in equimolar amounts for enzymatic activity. Protein B1 contains four binding sites for effector molecules in addition to two substrate binding sites with redox-active sulfhydryl groups. Protein B2 participates in the enzymatic reaction via a tyrosyl free radical that is formed in conjunction with a binuclear iron center. The tyrosyl radical appears to be a common feature of all iron-containing ribonucleotide reductases, and it has been demonstrated in the enzymes from such diverse sources as T4 bacteriophage, mouse 3T6 cells (Åkerblom et al., 1981), and mouse L cells infected with pseudorabies virus (Lankinen et al., 1982). The tyrosyl radical is believed to be the functional counterpart of cobalamin, which is the cofactor in a different class of ribonucleotide reductases found in organisms such as *Lactobacillus leichmanii*, *Rhizobium meliloti*, and *Euglenophyta*.

The tyrosyl radical of protein B2 can be selectively reduced by treatment with hydroxyurea, which causes a concomitant loss of enzymatic activity but does not alter the properties of the binuclear iron center (Atkin et al., 1973). The radical also disappears when the iron is removed by chelating agents. It is re-formed when apoprotein B2 is reconstituted with Fe(II) in the presence of O_2 (Petersson et al., 1980). The binuclear iron center in both native and radical-free protein B2 has been shown to consist of a pair of antiferromagnetically coupled, high-spin Fe(III) ions with magnetic and spectroscopic properties similar to those of the binuclear iron center of the oxygen transport protein hemerythrin (Atkin et al., 1973; Petersson et al., 1980; Loehr & Loehr, 1979). Thus, the binuclear iron center in protein B2 may serve the function of binding molecular oxygen and activating it for the abstraction of electrons from tyrosine residues.

The structure of the binuclear iron center in the Fe(III) form of hemerythrin has been elucidated by X-ray crystallography (Stenkamp & Jensen, 1979; Hendrickson, 1981). The current interpretation for methemerythrin azide is that the two iron atoms are coordinated to protein imidazolates and are bridged by two protein carboxylates and an oxo group from solvent (Stenkamp et al., 1981). The μ-oxo bridge is believed to be responsible for the strong antiferromagnetic interaction between the ferric ions as well as the intense electronic absorption bands in the near-UV spectra of methemerythrins and oxyhemerythrin (Garbett et al., 1969). In view of the strong similarities in the electronic spectra, Mössbauer spectra, and magnetic susceptibility between hemerythrin and protein B2, we were encouraged to seek additional evidence for a μ-oxo-bridged structure in protein B2.

Resonance Raman spectra of methemerythrins have revealed a vibrational mode near 510 cm^{-1}, which has been assigned to the stretching vibration of an Fe–O–Fe or Fe–O moiety on the basis that exchange with solvent oxygen ($H_2{}^{18}O$) leads to an ~15-cm^{-1} decrease in vibrational frequency (Freier et al., 1980). We discovered what appeared to be a similar vibrational mode at approximately 500 cm^{-1} in the resonance Raman spectra of native and radical-free protein B2 (Sjöberg et al., 1980). The results of isotopic substitutions with $H_2{}^{18}O$ and D_2O reported in this paper show that the ~500-cm^{-1} vibration in protein B2 is associated with an oxygen atom derived from solvent and that the rate of exchange is compatible with a μ-oxo-bridged formulation.

Experimental Procedures

Ribonucleotide Reductase. The *E. coli* B2 subunit was prepared and assayed for activity as described by Eriksson et al. (1977). The radical-free form of protein B2 was obtained

† From the Medical Nobel Institute, Department of Biochemistry, Karolinska Institute, S-104 01 Stockholm, Sweden (B.M.S.), the Department of Chemistry and Biochemical Sciences, Oregon Graduate Center, Beaverton, Oregon 97006 (T.M.L.), and the Department of Chemistry, Portland State University, Portland, Oregon 97207 (J.S.L.). *Received June 9, 1981.* This work was supported by grants from the Swedish Medical Research Council, the Magnus Bergvall Foundation, the Medical Faculty of the Karolinska Institute, and the U.S. Public Health Service, National Institutes of Health (GM 18865).

[1] Abbreviations: DNA, deoxyribonucleic acid; dCDP, deoxycytidine 5′-diphosphate; dATP, deoxyadenosine 5′-triphosphate; Tris, tris(hydroxymethyl)aminomethane; CD, circular dichroism; NMR, nuclear magnetic resonance.

0006-2960/82/0421-0096$01.25/0

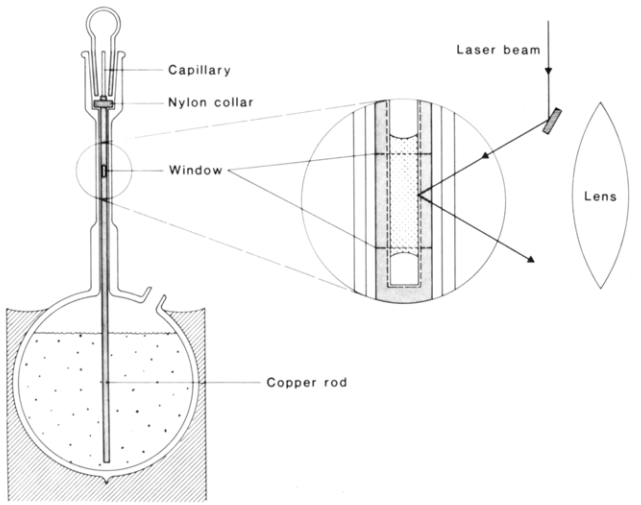

FIGURE 1: Dewar and cold-finger sample holder for low temperature control of capillary tubes. In detail at right copper rod is turned by 90°; illumination of the sample (crosshatched area within capillary) and light collection are in a backscattering geometry. The Dewar is 36-cm high and can hold 1 L of coolant.

by treatment with hydroxyurea (Sjöberg et al., 1980). Apoprotein B2 was prepared by treatment of the native protein with the iron chelator 8-hydroxyquinoline-5-sulfonate in the presence of 1 M imidazole and 10 mM hydroxylamine (Atkin et al., 1973).

Phage T4 induced β_2 protein was isolated in the iron-free form (Berglund, 1975) and reconstituted by the addition of iron(II) ascorbate and oxygen (Atkin et al., 1973) to yield a specific activity of 2000 units/mg. A unit of activity is the amount of T4β_2 that catalyzes the formation of 1 nmol of dCDP/min at 25 °C in the presence of excess T4α_2. Active and radical-free forms of T4β_2 were separated by chromatography on dATP–Sepharose upon elution with 10 mM Tris (pH 7.6)–20% glycerol (Eriksson et al., 1977); the radical-free form contained only 0.9 mol of Fe/mol of β_2. All protein samples were stored at −70 °C in 50 mM Tris-HCl–20% glycerol (pH 7.6).

Raman Samples. Ammonium sulfate precipitates were prepared by making the protein samples 60% saturated in $(NH_4)_2SO_4$ in 50 mM Tris-HCl (pH 7.6). After 5-min centrifugation at 13000*g*, the supernatant was carefully removed and the pellet was subjected to one or two additional centrifugations to eliminate as much liquid from the sample as possible. The final pellet, which was ~1 mM in protein, was drawn into an open-ended glass capillary (~1-mm i.d.) to a height of 10 mm, leaving a few millimeters of empty space below the sample. Slow freezing was accomplished by touching the end of the capillary to a copper rod immersed in liquid N_2. The frozen sample could then be inserted into the copper rod for spectral measurements (Figure 1) or stored in liquid N_2. However, rapid freezing of samples in liquid nitrogen gave poorer quality spectra.

Isotope exchange experiments were performed with $H_2{}^{18}O$ (99 atom %) and D_2O (99.8 atom %) obtained from Norsk Hydro, Norway. For exchange prior to reconstitution of native B2, apoprotein B2 (0.09 mL) was passed through a 1-mL Sephadex G-25 column equilibrated with 50 mM Tris-HCl (pH 7.6) in $H_2{}^{18}O$ or D_2O, reconstituted by the addition of iron(II) ascorbate, and precipitated by the addition of ammonium sulfate to 60% saturation. The protein in $H_2{}^{18}O$ was precipitated with solid $(NH_4)_2SO_4$ while the protein in D_2O was precipitated with a saturated solution of $(ND_4)_2SO_4$ in D_2O, prepared by lyophilizing ammonium sulfate from a D_2O solution and redissolving it in D_2O. Radical-free B2 was formed by the addition of hydroxyurea prior to ammonium sulfate precipitation. The extent of isotopic substitution was determined by mass spectrometry to be ~70% $H_2{}^{18}O$ or ~50% D_2O in the reconstituted samples. Raman experiments showed that the protein had completely exchanged with solvent in the 2–4 h required for reconstitution.

The kinetics of oxygen isotope exchange were studied by resuspending ~10 μL of hard-packed, H_2O-equilibrated ammonium sulfate pellet in 100 μL of $H_2{}^{18}O$, followed by the immediate addition of solid $(NH_4)_2SO_4$ to give 60% saturation or by resuspending 10 μL of $H_2{}^{18}O$-equilibrated pellet in 200 μL of 60% saturated $(NH_4)_2SO_4$ in H_2O. The ammonium sulfate precipitates were incubated at 4 °C, then centrifuged, and frozen in sample capillaries as described above. Exchange times refer to total time at 4 °C prior to freezing. Deuterium isotope exchange was performed as above with 10 μL of H_2O-equilibrated pellet being resuspended in 200 μL of 60% saturated $(ND_4)_2SO_4$ in D_2O. Mass spectral analyses showed ~80% $H_2{}^{18}O$, ~90% H_2O, and ~70% D_2O, respectively, in the exchange kinetics samples.

Raman Spectroscopy. Raman spectra were recorded on a computerized Jarrell-Ash spectrophotometer as described previously (Loehr et al., 1979). Excitation at 413.1, 406.7, and 356.4 nm was achieved with a Spectra-Physics Model 164-01 Kr ion laser equipped with a high-field magnet; the desired laser line was isolated by a Pellin-Broca prism monochromator (Instruments SA, Inc.). Scattered light was detected on a cooled ITT FW-130 (S-20) photomultiplier whose output was processed in an ORTEC Model 9302 amplifier/discriminator. Sample capillaries were irradiated in a quasi-backscattering geometry inside a copper rod cold finger immersed in liquid N_2 (Figure 1). Since previous experience had shown that native B2 protein was slowly damaged by UV laser irradiation, sample exposure time was minimized by blocking the light beam at all times except the ~1 min required for alignment and the 2.7 min required to scan from 400 to 670 cm^{-1} and from 900 to 1000 cm^{-1}. The latter region was used to check the internal sulfate vibration at 981 cm^{-1}. After ~10-min exposure, the capillary was repositioned to place a different area of the sample in the laser beam. The activity of native B2 samples following laser irradiation was 60–100% of the nonirradiated controls. Although the actual activity of the irradiated portion of the sample is difficult to determine, there was a general correlation between Raman spectral intensity and enzymatic activity. The less active samples gave weaker peaks (relative to the $SO_4{}^{2-}$ lines) but no changes in peak positions.

The extent of isotope exchange was determined by resolving the Raman spectral profiles into peaks of constant width (14 cm^{-1}) at half-maximal height and comparing the peak heights. Peak heights were corrected for Raman spectral contributions from buffer components and from residual H_2O or $H_2{}^{18}O$ (based on mass spectral analysis). The rate constant for oxygen isotope exchange was determined from the relationship $-\ln(1 - F) = k_{obsd}t$, where F (fraction exchanged) $= I_{481}/(I_{481} + I_{496})$ for exchange into $H_2{}^{18}O$ and $F = I_{496}/(I_{481} + I_{496})$ for back-exchange into $H_2{}^{16}O$. Peak positions are accurate to ±2 cm^{-1} for *E. coli* protein B2 and ±4 cm^{-1} for T4β_2 (for which much less protein was available).

Circular Dichroism Spectroscopy. CD spectra were recorded from 260 to 178 nm on a vacuum ultraviolet CD spectrophotometer as described by Hennessey & Johnson (1981). Samples were measured in 50-μm path length cells at ~5 °C with protein concentrations of 5.6 mmol of amino

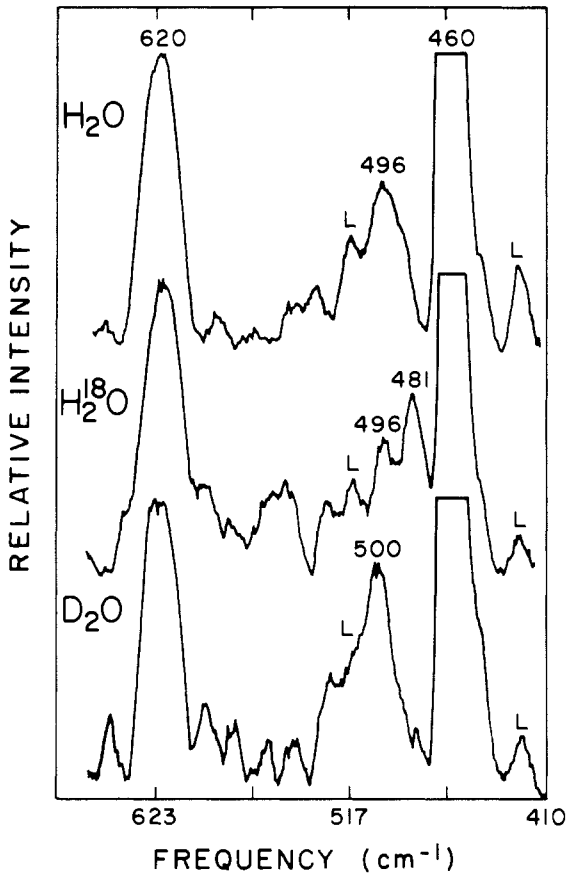

FIGURE 2: Resonance Raman spectra of native protein B2 of *E. coli* ribonucleotide reductase in solvents of different isotope composition. (Upper) Protein in H_2O; (middle) protein exposed to 75% $H_2^{18}O$ for 0.6 h at 4 °C; (lower) protein exposed to 70% D_2O for 1.1 h at 4 °C. The protein samples exhibited 50–60% of the activity of untreated samples at the end of the Raman experiment. The spectra were obtained with ~15 mW of 406.7-nm excitation and are accumulations of four, six, and six scans, respectively; scan rate 2.0 cm^{-1} s^{-1}, slit width ~10 cm^{-1}. Spectra have been subjected to background subtraction and a 25-point smooth. Laser plasma lines are denoted by L; an additional one is present underneath the 460-cm^{-1} sulfate peak.

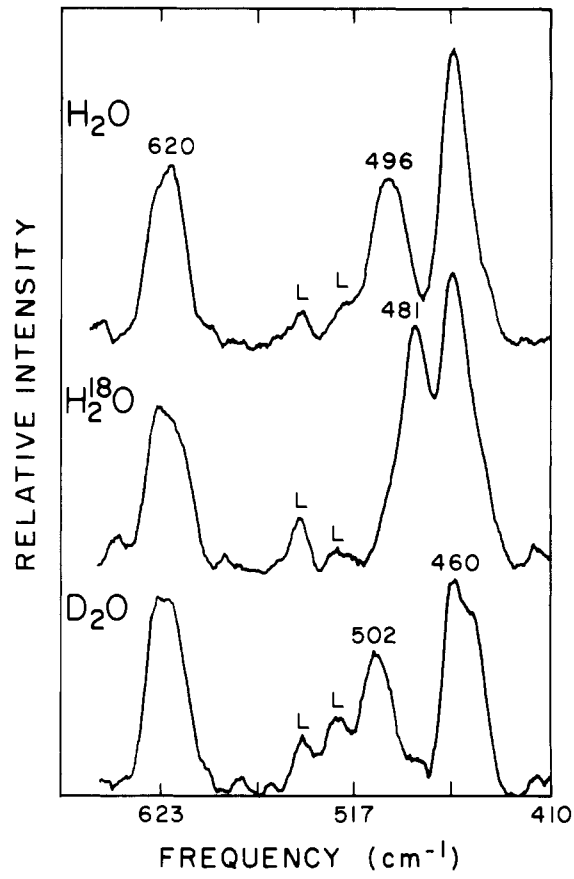

FIGURE 3: Resonance Raman spectra of radical-free protein B2 of *E. coli* ribonucleotide reductase in solvents of different isotope composition. (Upper) Protein in H_2O; (middle) protein reconstituted in 70% $H_2^{18}O$ and exposed for 2.5 h at 4 °C; (lower) protein reconstituted in 60% D_2O and exposed for 3.5 h at 4 °C. The spectra were obtained with ~15 mW of 413.1-nm excitation and are accumulations of three, three, and seven scans, respectively. Additional details as in legend to Figure 2.

acid/L (B2 protein) and 7.8 mmol of amino acid/L (B1 protein). CD intensities were rechecked at the end of each spectrum to make sure no sample decomposition had occurred during UV irradiation. The proteins were dissolved in deaerated 0.05 M potassium phosphate (pH 7.6) and contained 0.2% residual glycerol. In addition, protein B1 contained 0.002 M dithiothreitol. The concentration of protein B2 was determined by hydrolysis and reaction with ninhydrin (Hennessey & Johnson, 1981); the concentration of protein B1 was determined from its absorbance at 280 nm; $E^{1\%}_{1cm}$ = 10.8 (Thelander, 1973).

Results

Resonance Raman Vibrational Modes. We recently demonstrated that the iron center of ribonucleotide reductase from *E. coli* exhibits a resonance-enhanced vibration at ~500 cm^{-1} (Sjöberg et al., 1980). This feature is present in the spectra of the native and radical-free forms of protein B2 and absent from the spectrum of apoprotein B2, which lacks both the radical and the iron center. Repetition of these experiments with greater care in minimizing exposure of samples to laser irradiation has yielded higher quality spectra with greater intensity in the resonance-enhanced peak (appearing reproducibly at 496 cm^{-1} in both native and radical-free B2) relative to the 620-cm^{-1} sulfate peak (Figures 2 and 3, upper spectra). Furthermore, in native B2 samples showing >90% activity at the end of the Raman spectrum, the intensity of the 496-cm^{-1} peak was close to that of radical-free B2. This proves that the feature of the iron center responsible for the 496-cm^{-1} vibration is present in the native protein as well as in the radical-free protein. The intensity of the 496-cm^{-1} peak decreased with exposure time in both cases, but the rate of loss was more rapid for native than radical-free B2 and was correlated with a decrease in enzymatic activity.

Variation of excitation wavelength showed that maximal intensity of the 496-cm^{-1} peak was achieved with 413.1-, 406.7-, and 356.4-nm excitation. The peak was barely visible with 476.5- and 488.0-nm exciting lines (Ar laser) and completely absent with 568.2- and 647.1-nm exciting lines. The similar enhancements from 406.7- and 356.4-nm excitation indicate that the intensity maximum probably coincides with the 370-nm electronic absorption band associated with the antiferromagnetically coupled iron center in protein B2 (Petersson et al., 1980).

Ribonucleotide reductase produced by T4 bacteriophage contains a β_2 subunit that is analogous to the bacterial B2 subunit in its content of two iron atoms and the presence of a tyrosyl radical (M. Sahlin, A. Ehrenberg, B. M. Sjöberg, unpublished results). Excitation at 406.7 nm results in the appearance of a resonance Raman peak at 487 ± 4 cm^{-1} in both a fully active sample and a radical-free sample (containing 0.9 mol of Fe/mol of β_2). This feature was not observed in the Raman spectrum of apoprotein β_2. The dependence of the 487-cm^{-1} vibration on the presence of Fe in the

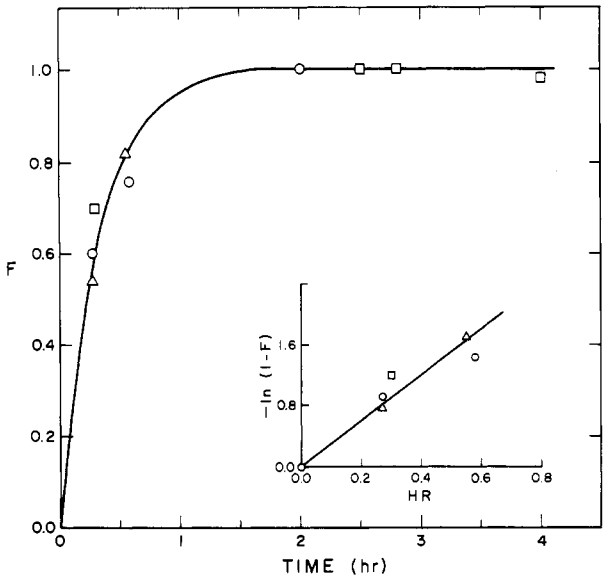

FIGURE 4: Rate of incorporation of oxygen from solvent into protein B2 at 4 °C in 60% ammonium sulfate. Native (○) and radical-free (□) protein B2 in H_2O transferred to $H_2{}^{18}O$; $F = I_{481}/(I_{481} + I_{496})$. Radical-free protein B2 in $H_2{}^{18}O$ transferred to H_2O (△); $F = I_{496}/(I_{481} + I_{496})$. Solid lines calculated for $k_{obsd} = 3.0\ h^{-1}$ from the relationship $-\ln(1 - F) = k_{obsd}t$.

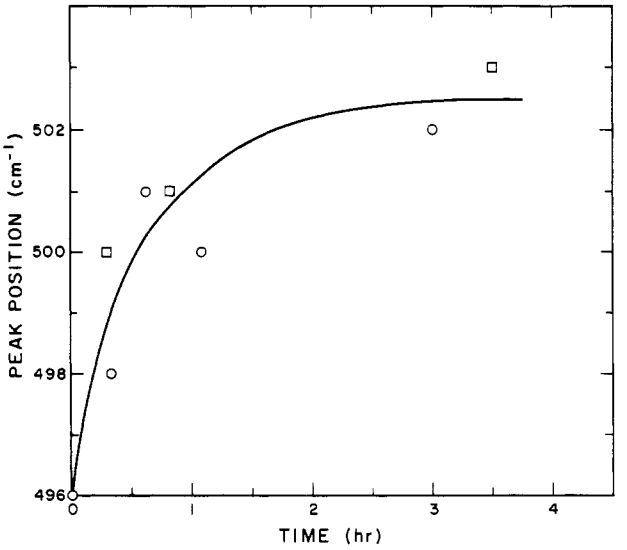

FIGURE 5: Frequency of Fe–O vibration as a function of time of exposure to D_2O. Ammonium sulfate precipitate of native (○) and radical-free (□) protein B2 resuspended in D_2O at 4 °C. Solid line represents best fit through data points.

sample and, presumably, an intact iron center makes it likely that this peak is analogous to the 496-cm^{-1} vibrational mode in bacterial protein B2.

Oxygen Isotope Exchange. When native or radical-free protein B2 is transferred from an H_2O-containing solvent to an $H_2{}^{18}O$-containing solvent, the iron-dependent vibrational mode shifts from 496 to 481 cm^{-1} (Figures 2 and 3, middle spectra). This shift clearly identifies the 496-cm^{-1} peak as an Fe–O vibrational mode and proves that the oxygen bound to iron can exchange with solvent oxygen. The assignment of this peak to an Fe–O vibration had been suggested earlier on the basis of the vibrational frequency and by analogy to the behavior of hemerythrin (Sjöberg et al., 1980).

As can be seen in Figure 2, the rate of oxygen exchange at 4 °C is slow enough that intermediate stages in the reaction can be observed at which both exchanged (481 cm^{-1}) and unexchanged (496 cm^{-1}) species are present. The relative intensities of the 481- and 496-cm^{-1} peaks (corrected for the isotope content of the solvent) were taken as a measure of the extent of oxygen exchange and are plotted in Figure 4 as a function of time of exposure to exchangeable solvent. The data can be fit by a first-order approximation and yield a pseudo-first-order rate constant of 3.0/h (or 8.3×10^{-4}/s). This analysis assumes that rates of exchange are similar for native and radical-free B2 and are independent of the direction of exchange.

Deuterium Exchange. The most likely possibilities for an exchangeable oxygen ligand are O^{2-}, OH^-, OH_2, and protein COO^-. If the ligand were OH^- or OH_2, replacement of H with D should cause the Fe–O vibration to shift to lower frequency in a manner similar to replacement with ^{18}O, whereas if the ligand were O^{2-} or COO^-, the spectrum should remain unchanged. Neither of these results was obtained when protein B2 was exposed to D_2O. Instead, the spectra of both native and radical-free B2 exhibited a gradual increase in the frequency of the 496-cm^{-1} peak to an apparent final value of 502 cm^{-1} (Figures 2 and 3, lower spectra). Another unusual aspect of the deuterium exchange reaction was that only a single sharp peak of intermediate frequency was observed at intermediate time points (e.g., the peak at 500 cm^{-1} in the lower, 1.1-h spectrum of Figure 2) with no indication of any residual component at 496 cm^{-1} (such as was observed with $H_2{}^{18}O$ in the middle spectrum of Figure 2). The peak width at half-maximum remained constant at 14 cm^{-1} throughout the exchange process, precluding the possibility that intermediate frequencies could represent a superpositioning of peaks at 496 and 502 cm^{-1}. The increase in frequency in D_2O is also greater than could be explained by the ±2-cm^{-1} error limit in frequency measurement in these samples.

The deuterium-dependent increase in the frequency of the Fe–O vibration with time of exposure to D_2O is shown in Figure 5. The deuterium exchange reaction appears to be occurring somewhat more slowly than the oxygen exchange reaction (Figure 4). Thus, it is unlikely that the deuterium reaction responsible for the increase in Fe–O vibrational frequency is due to a deuterium attached to an exchangeable oxygen. The most likely explanation for the deuterium effect is a gradual protein conformational change close to the iron center due to the substitution of protein hydrogen atoms by deuterium atoms.

Circular Dichroism. In view of the strong similarities between the binuclear iron centers in ribonucleotide reductase and hemerythrin, it was also of interest to determine whether there are similarities in protein structure. In hemerythrin the binuclear iron center is positioned inside four roughly parallel sections of the α helix (Stenkamp & Jensen, 1979). Both circular dichroism spectroscopy and X-ray crystallography reveal that about 70% of the amino acid residues in hemerythrin are in α-helical regions (Darnall et al., 1969). Circular dichroism spectra of the B1 and B2 proteins of ribonucleotide reductase are shown in Figure 6. Comparison with the circular dichroism spectra of proteins and polypeptides of known structure (Chen et al., 1972; Greenfield & Fasman, 1969) leads to an estimate of ~60% α helix for protein B2 and ~40% α helix for protein B1. The lower helical content for protein B1 is consistent with the catalytic and regulatory function of this subunit, whereas the higher helical content for protein B2 is more typical of proteins such as hemoglobin and hemerythrin that have no real catalytic function.

The high α-helical content of protein B2 offers the possibility for a protein structure at the binuclear iron center that is similar to that of hemerythrin. However, there is a great difference in size per binuclear iron center: hemerythrin has

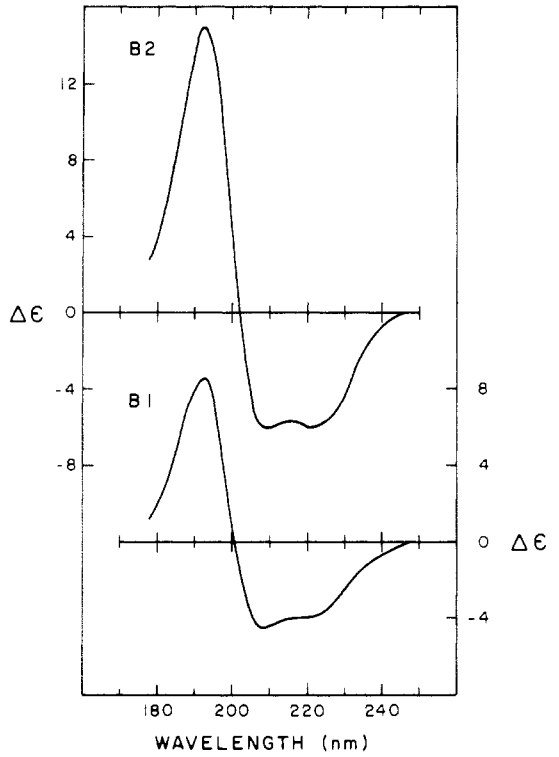

FIGURE 6: Circular dichroism spectra of B2 and B1 subunits of *E. coli* ribonucleotide reductase.

a molecular weight of 13 400 (Loehr et al., 1978) whereas protein B2 has a molecular weight of 78 000 (Thelander, 1973). Furthermore, since protein B2 is composed of two apparently identical polypeptide chains, the binuclear iron center is probably located at a subunit interface.

Discussion

In our previously reported study of the B2 subunit of ribonucleotide reductase, we concluded that the iron-dependent peak at $\sim$500 cm^{-1} was most likely due to an Fe–O vibration with the oxygen derived either from solvent (H_2O, OH^-, or μ-oxo) or from a protein carboxylate (Sjöberg et al., 1980). The sensitivity of the 496-cm^{-1} peak of protein B2 to oxygen isotope substitution in the present study confirms its assignment as an Fe–O vibrational mode and enables us to distinguish between the above possibilities. The spectral shift to 481 cm^{-1} in $H_2{}^{18}O$ is in the expected direction for an increase in mass of the vibrating system. However, the observed 15-cm^{-1} shift is smaller than the 22-cm^{-1} shift predicted for a pure Fe–O stretching vibration on the basis of mass considerations alone, indicating that additional structural components are contributing to this vibrational mode.

The oxygen exchange rate in protein B2, as determined from the rate of change in the Raman spectral intensities at 496 and 481 cm^{-1}, makes it improbable that carboxylate is the oxygen donor. Exchange of carboxylate oxygens is considerably slower than the observed exchange in protein B2, and it is acid catalyzed (Table I). At the pH of 7.6 used in the protein experiments, carboxylate-oxygen exchange would be exceedingly slow and could not account for the observed rate in protein B2 unless there were catalysis by acidic functional groups close to the iron center. Conversely, the exceedingly rapid rates of H_2O exchange in aquo complexes (Table I) make H_2O an unlikely candidate for the Fe–O species in protein B2. Hydroxo exchange may be up to 50 times slower than aquo exchange, as in $[Co(NH_3)_5OH]^{2+}$ (Hunt & Taube, 1958) and $[Co(PDTA)OH]^{2-}$ (Swaminathan & Busch, 1962), but would still be many orders of magnitude faster than the rate observed for protein B2. The data that comes closest to accounting for the oxygen exchange behavior of protein B2 is that of the μ-oxo-bridged iron complexes (Table I). The $\sim 10^3$-fold slower exchange in protein B2 could be due, in part, to the lower temperature and precipitated state of the protein but also to additional factors such as lower solvent accessibility and greater stability of the iron center than in the inorganic complexes. Bulky ligands that increase the size of a metal complex are known to decrease the rate of ligand exchange, presumably by decreasing the ease of solvation (Basolo & Pearson, 1967).

The deuteration results with protein B2 also favor the formulation of a μ-oxo structure over that of an aquo or hydroxo species. Metal–oxygen stretching vibrations are generally shifted 10–25 cm^{-1} to lower frequency when the hydrogen in M–OH is replaced by deuterium (Table II). For protein B2, no shift to lower frequency was observed in D_2O. Instead, the Fe–O vibration at 496 cm^{-1} gradually increased in frequency with time until it reached a maximum value of 502 cm^{-1}. We attribute this increase in frequency to a gradual structural alteration in the iron center resulting from changes

Table I: Rate Constants for Exchange of Metal-Coordinated Oxygen with Solvent Oxygen

complex	k (s^{-1})	reference
carboxylate[a]		
$[Co(NH_3)_5$formate$]^{2+}$		
0.5 M HCl	1.5×10^{-5}	Andrade et al. (1970)
0.05 M HCl	3.0×10^{-6}	Andrade et al. (1970)
$[Co(NH_3)_5$acetate$]^{2+}$, 0.5 M HCl	$<3 \times 10^{-8}$	Andrade et al. (1970)
$[Cr(oxalate)_3]^{3+}$, neutral pH	no exchange	Bunton et al. (1964)
$[Ni(iminodiacetate)_2]^{2-}$, 0.1 M $HClO_4$	$<1 \times 10^{-7}$	Connick (personal communication)
aquo[b]		
$[Fe(H_2O)_6]^{3+}$	2.4×10^{4}	Connick & Stover (1961)
$[Fe(H_2O)_6]^{2+}$	3.2×10^{6}	Swift & Connick (1962)
$[Co(H_2O)_6]^{2+}$	1.1×10^{6}	Swift & Connick (1962)
$[Ni(H_2O)_6]^{2+}$	2.7×10^{4}	Swift & Connick (1962)
μ-oxo[c]		
$[Fe_2(EDTA)_2O]^{4-}$	1.2	Wilkins & Yelin (1969)
$[Fe_2(HEDTA)_2O]^{2-}$	4.0	Wilkins & Yelin (1969)
$[Fe_2(CyDTA)_2O]^{4-}$	9	Wilkins & Yelin (1969)
$[Fe_2(TPPS)_2O]^{8-}$	41	Fleischer et al. (1971)
di-μ-oxo[d]		
$[Mo_2O_4]^{2+}_{aq}$	4.7×10^{-7}	Murmann (1980)
$[Mo_3O_4]^{4+}_{aq}$	$<3 \times 10^{-7}$	Murmann & Shelton (1980)
protein B2[e]	8.3×10^{-4}	this work

[a] k at 25 °C for exchange with $H_2{}^{18}O$ in Cr and Co complexes; from ^{17}O NMR in Ni complex. [b] k from NMR relaxation of ^{17}O in 0.1 M $HClO_4$ at 25 °C. [c] k for acid-independent dissociation at 25 °C, the rate-limiting step in oxygen exchange. EDTA = ethylenediaminetetraacetate; HEDTA = hydroxyethylethylenediaminetriacetate; CyDTA = 1,2-cyclohexanediaminetetraacetate; TPPS = tetrasulfonated tetraphenylporphine. [d] k for exchange with $H_2{}^{18}O$ in 0.3–3 M HCl at 25 °C. [e] k for exchange with $H_2{}^{18}O$ in 60% saturated ammonium sulfate–0.1 M Tris (pH 7.6) at 4 °C.

Table II: Hydrogen Isotope Dependence of Metal–Oxygen Vibrational Frequencies (cm^{-1})

complex	solvent H_2O	solvent D_2O	Δ	reference
$As(OH)_3$	710	690	−20	Loehr & Plane (1968)
$[Cr_2(NH_3)_{10}(OH)]^{5+}$	569	549	−20	Hewkin & Griffith (1966)
$[PtCl_4(OH)_2]^{2-}$	548	537	−11	Cox & Peters (1970)
$[VO_3(OH)]^{2-}$	545	520	−25	Griffith & Wickens (1966)
$[OsO_4(OH)_2]^{2-}$	520	505	−15	Griffith (1964)
protein B2	496	502	+6	this work

in protein conformation. Deuteration could also influence hydrogen-bonding interactions with the oxo group. Sensitivity to D_2O has been observed in a number of regulatory proteins and is believed to be due to alterations in the conformation or degree of aggregation of subunits (Henderson et al., 1970). In ribonuclease, the $t_{1/2}$ for the exchange of peptide hydrogens at 4 °C, pH 4.7, varies from 8 to 160 min depending upon their degree of hydrogen bonding, whereas functional-group hydrogen exchange is complete in less than 2 min (Englander, 1967). As the rate of exchange would be faster at pH 7.6, the $t_{1/2}$ of 22 min for the 496–502-cm^{-1} shift in protein B2 indicates that the conformational changes resulting from deuteration would have to be due to fairly inaccessible peptide and/or functional group hydrogens.

The resonant behavior of the 496-cm^{-1} vibrational mode in the B2 protein requires that the 370-nm electronic transition associated with this intensity enhancement have considerable O → Fe(III) charge-transfer character. Such dependency is well documented for bridging and terminal oxo groups in $Fe_2(TPP)_2O$, $(Os_2Cl_{10}O)^{4-}$, $(Ru_2Cl_{10}O)^{4-}$, CrO_4^{2-}, and MnO_4^- (Burke et al., 1978; San Fillipo et al., 1976; Clark & Steward, 1979). However, these species owe much of their electronic charge-transfer properties and the resulting strongly enhanced Raman intensities to good π overlap in their linear M–O or M–O–M bonds. This capacity would be diminished if a bent M–O–M system is present in protein B2 (see below). Nevertheless, the resonance-enhanced Fe–O vibration in protein B2 is more likely to be due to μ-oxo-bridged Fe's, which are known to have strong UV absorptions (Murray, 1974), than to aquo, hydroxylato, or carboxylato complexes, which are much weaker chromophores.

Identification of the 496-cm^{-1} peak of protein B2 with a stretching vibration of an Fe–O–Fe system would also account for the low value of 15 cm^{-1} for the frequency shift in $H_2{}^{18}O$. In a singly bridged system the location of a symmetric stretch close to 500 cm^{-1} is indicative of a bent M–O–M structure, and in such a structure the extent of the shift in $H_2{}^{18}O$ is inversely related to the M–O–M angle (King & Callahan, 1969). Thus, the observed shift from 496 to 481 cm^{-1} gives a calculated Fe–O–Fe angle of 132° for protein B2. Alternatively, the smallness of the isotope shift in protein B2 could be due to the location of the iron atoms in a triply bridged structure as in hemerythrin (Stenkamp et al., 1981). Methemerythrins exhibit an analogous shift of ~15 cm^{-1} in the ~507-cm^{-1} Fe–O–Fe vibration when they are exchanged with $H_2{}^{18}O$ (Freier et al., 1980). For both protein B2 and methemerythrins (J. D. McCallum, T. M. Loehr, and J. Sanders-Loehr, unpublished results) maximal enhancement of the 496- and 507-cm^{-1} Fe–O vibration, respectively, occurs with ~370-nm excitation, indicating that similar electronic transitions are responsible for intensity enhancement. The 507-cm^{-1} peak in methemerythrin is also enhanced by 530-nm excitation (Dunn et al., 1977); this has not been observed for the 496-cm^{-1} peak of ribonucleotide reductase. Thus, there must be some differences in the electronic and molecular structures of the iron centers in the two proteins.

A striking difference between protein B2 of ribonucleotide reductase and hemerythrin is in the conditions required for exchange of the endogenous iron-bound oxygen. Whereas the exchange rate in protein B2 is facile and compatible with an Fe–O–Fe structure (Table I and above discussion), the oxygen responsible for the Fe–O vibration in methemerythrin does not exchange with solvent; exchange is observed only during the displacement of bound O_2 from oxyhemerythrin by the exogenous ligands N_3^-, CN^-, or OCN^- (Freier et al., 1980). Since the exchangeable oxygen only becomes accessible during the expulsion of bound O_2, it would appear that the Fe–O–Fe moiety in hemerythrin is more highly constrained than in protein B2. One such possibility is that although the two iron atoms in hemerythrin are multiply bridged (Stenkamp et al., 1981), the two iron atoms in protein B2 are bridged by only a single μ-oxo group. In support of this likelihood, the multiply bridged Mo complexes in Table I show greatly reduced rates of oxygen exchange compared to singly bridged μ-oxo complexes. Alternatively, the oxygen attached to the dimeric iron complex in hemerythrin might be prevented from dissociating by a greater structural rigidity of the protein. Although circular dichroism of protein B2 shows that it contains almost as much α helix as hemerythrin, the iron atoms in protein B2 appear to be located at a subunit interface. A similar structure has been proposed for the iron binding sites in apoferritin (Banyard et al., 1978).

Acknowledgments

We are grateful to John Hennessey and Gary Causley of Oregon State University for their help in obtaining the circular dichroism spectra and to Björn Lindström of the National Board of Health and Welfare, Uppsala, Sweden, for the mass spectroscopic determinations.

References

Åkerblom, L., Ehrenberg, A., Gräslund, A., Lankinen, H., Reichard, P., & Thelander, L. (1981) *Proc. Natl. Acad. Sci. U.S.A. 78*, 2159.

Andrade, C., Jordan, R. B., & Taube, H. (1970) *Inorg. Chem. 9*, 711.

Atkin, C. L., Thelander, L., Reichard, P., & Lang, G. (1973) *J. Biol. Chem. 248*, 7464.

Banyard, S. H., Stammers, D. K., & Harrison, P. M. (1978) *Nature (London) 271*, 282.

Basolo, F., & Pearson, R. G. (1967) *Mechanisms of Inorganic Reactions*, p 161, Wiley, New York.

Berglund, O. (1975) *J. Biol. Chem. 250*, 7450.

Bunton, C. A., Carter, J. H., Llewellyn, D. R., O'Connor, C., Odell, A. L., & Yih, S. Y. (1964) *J. Chem. Soc.*, 4615.

Burke, J. M., Kincaid, J. R., & Spiro, T. G. (1978) *J. Am. Chem. Soc. 100*, 6077.

Chen, Y. H., Yang, J. T., & Martinez, H. M. (1972) *Biochemistry 11*, 4120.

Clark, R. J. H., & Stewart, B. (1979) *Struct. Bonding (Berlin) 36*, 1.

Connick, R. E., & Stover, E. D. (1961) *J. Phys. Chem. 65*, 2075.

Cox, L. E., & Peters, D. G. (1970) *Inorg. Chem. 9*, 1927.

Darnall, D. W., Garbett, K., Klotz, I. M., Atkipis, S., & Keresztes-Nagy, S. (1969) *Arch. Biochem. Biophys. 133*, 103.

Dunn, J. B. R., Addison, A. W., Bruce, R. E., Loehr, J. S., & Loehr, T. M. (1977) *Biochemistry 16*, 1743.

Englander, S. W. (1967) in *Poly α-Amino Acids* (Fasman, G. D., Ed.) p 339, Marcel Dekker, New York.

Eriksson, S., Sjöberg, B.-M., Hahne, S., & Karlström, O. (1977) *J. Biol. Chem. 252*, 6132.

Fleischer, E. B., Palmer, J. M., Srivastava, T. S., & Chatterjee, A. (1971) *J. Am. Chem. Soc. 93*, 3162.

Freier, S. M., Duff, L. I., Shriver, D. F., & Klotz, I. M. (1980) *Arch. Biochem. Biophys. 205*, 449.

Garbett, K., Darnall, D. W., Klotz, I. M., & Williams, R. J. P. (1969) *Arch. Biochem. Biophys. 135*, 419.

Greenfield, N., & Fasman, G. D. (1969) *Biochemistry 8*, 4108.

Griffith, W. P. (1964) *J. Chem. Soc.*, 245.

Griffith, W. P., & Wickins, T. D. (1966) *J. Chem. Soc. A*, 1087.
Henderson, R. F., Henderson, T. R., & Woodfin, B. M. (1970) *J. Biol. Chem. 245*, 3733.
Hendrickson, W. A. (1981) in *Invertebrate Oxygen-Binding Proteins: Structure, Active Site, and Function* (Lamy, J., & Lamy, J., Eds.) p 503, Marcel Dekker, New York.
Hennessey, J. P., Jr., & Johnson, W. C., Jr. (1981) *Biochemistry 20*, 1085.
Hewkin, D. J., & Griffith, W. P. (1966) *J. Chem. Soc. A*, 472.
Hunt, H. R., & Taube, H. (1958) *J. Am. Chem. Soc. 80*, 2642.
King, R. M., & Callahan, K. P. (1969) *Inorg. Chem. 8*, 871.
Lankinen, H., Gräslund, A., & Thelander, L. (1982) *J. Virol.* (in press).
Loehr, J. S., & Loehr, T. M. (1979) *Adv. Inorg. Biochem. 1*, 235.
Loehr, J. S., Lammers, P. J., Brimhall, B., & Hermodson, M. A. (1978) *J. Biol. Chem. 253*, 5726.
Loehr, T. M., & Plane, R. A. (1968) *Inorg. Chem. 7*, 1708.
Loehr, T. M., Keyes, W. E., & Pincus, P. A. (1979) *Anal. Biochem. 96*, 456.
Murmann, R. K. (1980) *Inorg. Chem. 19*, 1765.
Murmann, R. K., & Shelton, M. E. (1980) *J. Am. Chem. Soc. 102*, 3984.
Murray, K. S. (1974) *Coord. Chem. Rev. 12*, 1.
Petersson, L., Gräslund, A., Ehrenberg, A., Sjöberg, B.-M., & Reichard, P. (1980) *J. Biol. Chem. 255*, 6706.
San Fillipo, J., Jr., Grayson, R. L., & Sniadoch, M. J. (1976) *Inorg. Chem. 15*, 269.
Sjöberg, B.-M., Gräslund, A., Loehr, J. S., & Loehr, T. M. (1980) *Biochem. Biophys. Res. Commun. 94*, 793.
Stenkamp, R. E., & Jensen, L. H. (1979) *Adv. Inorg. Biochem. 1*, 219.
Stenkamp, R. E., Sieker, L. C., Jensen, L. H., & Sanders-Loehr, J. (1981) *Nature (London) 291*, 263.
Swaminathan, K., & Busch, D. H. (1962) *Inorg. Chem. 1*, 256.
Swift, T. J., & Connick, R. E. (1962) *J. Chem. Phys. 37*, 307.
Thelander, L. (1973) *J. Biol. Chem. 248*, 4591.
Thelander, L., & Reichard, P. (1979) *Annu. Rev. Biochem. 48*, 133.
Wilkins, R. G., & Yelin, R. E. (1969) *Inorg. Chem. 8*, 1470.

Fluorometric Studies on the Binding of Gluconolactone, Glucose, and Glucosides to the Subsites of Glucoamylase†

Keitaro Hiromi,* Akiyoshi Tanaka, and Masatake Ohnishi

ABSTRACT: Static studies were made at pH 4.5 and 10 °C on the binding of *Rhizopus niveus* glucoamylase with four kinds of substrate analogues, i.e., gluconic acid 1,5-lactone (gluconolactone), glucose, methyl α-glucoside, and phenyl β-glucoside, by monitoring the enzyme fluorescence decrease caused by the ligand binding. The dissociation constant (K_d) and the percentage of maximum decrease of fluorescence intensity (ΔF_{max}) for the binary complex formation between these ligands and the enzyme were evaluated. Among these analogues, gluconolactone showed the smallest K_d value (1.1 mM) and the largest ΔF_{max} value (30%). From the fluorometric titration of the enzyme with gluconolactone in the presence of glucose or the glucosides, it was found that gluconolactone and glucose (or the glucosides) can bind to the enzyme simultaneously to form a ternary enzyme–gluconolactone–glucose (or -glucoside) complex. The percentage of maximum decrease of the fluorescence intensity caused by the ternary complex formation (about 30%) is almost equal to that observed for the binary enzyme–gluconolactone complex formation. The dissociation constant of gluconolactone from the ternary complex was considerably smaller (about a factor of 0.3) than that from the enzyme–gluconolactone complex. These results, together with the information obtained so far, lead to the following conclusions: (1) Gluconolactone binds to subsite 1 of the enzyme active site, where the nonreducing-end glucose residue of a substrate is bound in a productive binding mode, and glucose and the glucose moiety of the glucosides bind to subsite 2. (2) The decrease of the enzyme fluorescence arises from one tryptophan residue, which is supposed to be located at or close to subsite 1. (3) There is a positive interaction between subsite 1 and subsite 2 as to decrease the dissociation constant for the ligand binding at each subsite.

Glucoamylase[1] successively hydrolyzes glucosidic bonds from the nonreducing end of the substrate starch to produce glucose. By steady-state kinetic studies, the subsite structure (the arrangement of the affinities of subsites for glucose residues of linear substrates) of *Rhizopus* glucoamylase has been estimated by Hiromi et al. (Hiromi, 1970; Hiromi et al., 1973). The subsites are numbered from the nonreducing end of the substrate bound in the productive mode, as shown in Figure 1, and the catalytic site is considered to be located between subsite 1 and subsite 2 (Hiromi et al., 1973). Since subsite 2 has the highest affinity, the glucose or glucose moiety of glucosides is considered to bind predominantly to subsite 2 (Ohnishi et al., 1975, 1976). The apparent zero value of the affinity of subsite 1 (Hiromi et al., 1973) has been interpreted to indicate that the decrease in free energy due to the specific interaction between the nonreducing terminal glucose residue and this subsite is counterbalanced by the free

† From the Department of Food Science and Technology, Faculty of Agriculture, Kyoto University, Kyoto 606, Japan. *Received April 28, 1981.* This work was supported in part by a grant-in-aid for Scientific Research from the Ministry of Education, Science and Culture of Japan (No. 447094).

[1] Abbreviations used: E or glucoamylase, 1,4-α-D-glucan glucohydrolase from *Rhizopus niveus* (EC 3.2.1.3); L or gluconolactone, gluconic acid 1,5-lactone; G, glucose or glucose residue of glucosides.

0006-2960/82/0421-0102$01.25/0